

Electroconvection in nematic mixtures of bent-core and calamitic molecules

Shingo Tanaka, Hideo Takezoe

*Department of Organic and Polymeric Materials, Tokyo Institute of Technology,
2-12-1 S8-Ookayama, Meguro-Ku, Tokyo, 152-8552 Japan*

Nándor Éber, Katalin Fodor-Csorba, Anikó Vajda, Ágnes Buka
Research Institute for Solid State Physics and Optics,

Hungarian Academy of Sciences, H-1525 Budapest, P.O.B. 49, Hungary

(Dated: April 16, 2009)

The onset of electroconvection in binary mixtures of a bent-core and a rod-like nematic has been characterized by measuring the threshold voltage U_c and the critical wave number of the pattern in a wide range of frequencies f . In the 'banana' rich mixtures a "conductive-prewavy2-patternless-prewavy1" morphological sequence has been detected with an unusual negative slope of $U_c(f)$ at high frequencies. This latter scenario seems to be related to the bent-core component, as it disappears with increasing the concentration of rod-like molecules. In addition, one of the parameters most relevant for electroconvection, the electrical conductivity, has also been varied by ionic salt doping. It has been found that the above effect of the banana shape molecules on the electroconvection scenarios can be suppressed by the conductivity.

PACS numbers: 47.54.-r, 61.30.Gd, 47.20.Lz

I. INTRODUCTION

Liquid crystals made of achiral bent core molecules have drawn considerable attention in the last decade due to their ability to form unconventional 'banana' phases, including those with polar packing and ferroelectric switching and those exhibiting spontaneous chiral domain segregation [1]. The bent molecular structure may, moreover, lead to extraordinary properties even in the conventional mesophases; e.g. bent core nematics are regarded as candidates for exhibiting a long searched biaxial nematic phase [2, 3]. A giant flexoelectricity [4] as well as some unprecedented behaviour of electroconvection patterns [5] have also been reported recently in a 'banana' nematic.

Electroconvection (EC) is a pattern forming instability of a homogeneous nematic liquid crystal layer which involves electric field induced director deformation with an associated charge separation and flow [6]. The resulting patterns have a great morphological richness. At onset they mostly appear in the form of regular convection rolls seen as stripes of varying intensity and/or colour in a polarising microscope. Their wave vector \mathbf{q} might cover a wide range depending on the material parameters of the nematic compound and on the frequency f and the rms value U of the applied voltage [7].

The most common examples of EC (the 'conductive' and the 'dielectric' rolls) are primarily observed in planar layers of calamitic nematics with negative dielectric and positive conductivity anisotropies ($\epsilon_a < 0$, $\sigma_a > 0$). They are called standard EC patterns as their mechanism of formation as well as their main characteristics (the threshold voltage U_c and the critical wave vector \mathbf{q}_c) are well described by the standard model (SM) of electroconvection (i.e. by the combination of equations of nematodynamics with electrodynamics assuming Ohmic

conduction) [8]. The two regimes of standard EC patterns differ in the temporal symmetries of their flow and director distortions, furthermore in $U_c(f)$ and $\mathbf{q}_c(f)$. At low f usually 'conductive' rolls are present characterized by a wavelength about the sample thickness d ($q_c \approx (1.5 - 3)\pi/d$); their $U_c(f)$ increases sharply with f when approaching a crossover frequency f_c , where the 'dielectric' rolls take over. The latter are usually thinner ($\lambda < 5 \mu\text{m}$) and independent of d ; their threshold voltage has a square root like frequency dependence. As for the direction of \mathbf{q}_c one has to distinguish between normal rolls (NR) which run perpendicular to the initial director \mathbf{n} ($\mathbf{q}_c \parallel \mathbf{n}$) and oblique rolls (OR) which run in two degenerate directions thus forming zig-zag structures (\mathbf{q}_c makes a small ($< 45^\circ$) angle with \mathbf{n}). OR are typical for the lowest frequencies; increasing f the obliqueness reduces and above the Lifshitz point f_L the pattern transforms into NR. The Lifshitz point falls usually in the 'conductive' regime, although oblique dielectric rolls have also been reported recently [9]. These types of patterns are also observable in homeotropically aligned cells as secondary instabilities above a bend Freedericksz transition [7, 10].

The calamitic nematics mentioned above occasionally exhibit a third type of morphology at onset: the 'prewavy' pattern (also called wide domains) [11–17]. It manifests itself in stripes much wider than d ($q_c < \pi/d$) and with $\mathbf{q}_c \parallel \mathbf{n}$. In contrast to 'conductive' or 'dielectric' NR, however, the 'prewavy' pattern is only visible with crossed polarisers. Its threshold U_c has weak, linear frequency dependence; therefore it can be detected at high frequencies. At increasing f a sequence of transitions from 'conductive' to 'dielectric' rolls and then to the 'prewavy' pattern has been reported [18]. A higher conductivity has been found to promote the formation of the 'prewavy' pattern by reducing its threshold; then a

direct transition from 'conductive' rolls to the 'prewavy' pattern is often observed [15]. The formation mechanism of this pattern has not been uncovered yet; it could not be explained within the framework of the SM.

Electroconvection could experimentally be detected in calamitic nematics even with $\varepsilon_a < 0$, $\sigma_a < 0$ [19–21]. Since the SM of EC predicts no instability for the case when the dielectric and the conductivity anisotropies are of the same sign, the observed patterns were classified as nonstandard EC [7, 21, 22]. The nonstandard rolls are visible with crossed polarisers only (like the 'prewavy' pattern), have a linear $U_c(f)$ behaviour and are longitudinal, i.e. run either parallel to the director ($\mathbf{q}_c \perp \mathbf{n}$) or are strongly oblique (\mathbf{q}_c makes a large ($> 60^\circ$) angle with \mathbf{n}). It has recently been understood that extending the SM by incorporating flexoelectric effects could provide finite threshold voltages for this case and could give an account of the experimental pattern characteristics [23].

Electroconvection may also occur in 'banana' nematics; however, only a few experiments have been reported so far [5, 24–27]. The compound 4-chloro-1,3-phenylene-bis-4-[4'-(9-decenyloxy) benzoxy] benzoate (**CIPbis10BB**) [5, 28] which has been tested in most detail, had $\varepsilon_a < 0$ and a conductivity anisotropy changing sign twice with the frequency ($\sigma_a < 0$ for low f and at high f , while $\sigma_a > 0$ at intermediate frequencies). At low f nonstandard longitudinal rolls have been seen as expected from the signs of the anisotropies. At increasing f , however, it has exhibited two 'prewavy' morphologies (PW1 and PW2) which have been separated by a frequency band where no patterns existed at all (refer to Fig. 2b). Their threshold voltages seemed to diverge hiperbolically when approaching this frequency band from any side; otherwise PW1 and PW2 had similar appearance (wavelength, direction, contrast). A similar behaviour has also been reported for another bent-core nematic compound [24]. The reason for these unusual features still awaits for exploration.

Mixing compounds of different chemical architecture has proved to be an effective tool to adjust the temperature range and some material parameters of calamitic liquid crystals. One expects that mixing might have similar advantages for bent core materials too; however, much less efforts have been devoted to such studies so far. Some early trials have indicated only limited miscibilities of 'banana' phases. Recently binary mixtures of 'banana' and calamitic nematics could successfully be prepared where the nematic phase could be preserved in the whole concentration range [29].

In the present paper we report about electroconvection measurements on these binary mixtures of bent core and calamitic nematics. In Section II we introduce the substances, the setup, and the measuring method. In Section III we aim to explore how does the dilution of the 'banana' nematic by a calamitic compound affect the electroconvection thresholds and morphologies. As the magnitude of the electrical conductivity may have a large influence on the EC behaviour, in Section IV we construe

the consequences of adjusting the conductivity of a selected mixture by doping it with an ionic salt. Finally, we conclude the paper with the discussion in Section V.

II. EXPERIMENTAL

The experiments have been carried out on binary mixtures of a bent-core and a calamitic nematic liquid crystal. The well characterized compound **CIPbis10BB** [28] has been selected as the bent-core component. As the calamitic constituent of the mixtures 4-n-octyloxy-phenyl-4'-n-hexyloxy-benzoate (**6008**) [30] has been chosen since its structure is similar to that of the arms of the bent-core compound. The chemical structures of these molecules are shown in Fig. 1. The selected compounds are known to exhibit full miscibility, possessing nematic phase at any concentration [29]. Mixtures with three different compositions have been prepared by thorough mixing of the components and letting to homogenize for an hour in the isotropic phase. The mixtures **7B3R**, **5B5R** and **3B7R** contained 70 wt%, 50 wt% and 30 wt% of the bent-core molecules, respectively. The phase sequences of these mixtures as well as that of the pure compounds are given in Table I.

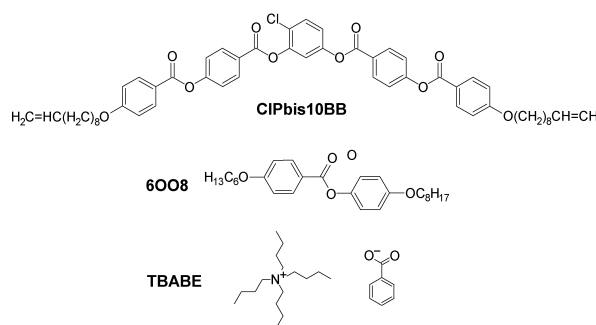


FIG. 1: Chemical structures of the bent-core **CIPbis10BB**, the rod-like **6008** molecules and the ionic salt **TBABE** used in the mixtures.

In order to modify the electrical conductivity of the mixture **7B3R** a doping by the ionic salt tetra butyl ammonium benzoate (**TBABE**) in concentrations of 0.01 wt%, 0.1 wt% and 1 wt%, respectively, has also been performed. The chemical structure of this dopant is also shown in Fig. 1. The salt was added to the mixture **7B3R** in a chloroform solution; after mixing it was kept at 60 °C for about 2 hours in order to let the solvent to evaporate. The measured electrical conductivities of the mixtures (when available) are given in Table I.

In the nematic phase, the dielectric anisotropy ε_a of both the bent-core **CIPbis10BB** and the rod-like **6008** are negative ($\varepsilon_a < 0$); the same holds for their mixtures too. The conductivity anisotropy σ_a has, however, a more delicate behaviour. As characterized by Wiant et al. [5], σ_a of **CIPbis10BB** changes from negative to positive and then again to negative as the frequency is

TABLE I: Composition, electrical conductivity (σ_{\perp} at 80 °C, 1 kHz) and phase sequence of the pure compounds and their mixtures. Cr, SmC, N and I denote crystalline, smectic C, nematic and isotropic phases, respectively; SmX is an unidentified smectic phase.

Name	CIPbis10BB (wt%)	6OO8 (wt%)	TBABE (wt%)	σ_{\perp} ($\Omega^{-1}m^{-1}$)	Phase sequence and transition temperatures on cooling (°C)
CIPbis10BB	100	0	0	$1.6 \cdot 10^{-7}$ [5]	Cr 60 N 78 I [5]
7B3R	70	30	0	$2.4 \cdot 10^{-8}$	SmX 48 SmC 70 N 88 I
			0.01	-	
			0.1	$7.5 \cdot 10^{-7}$	
			1	$7.5 \cdot 10^{-6}$	
5B5R	50	50	0	-	Cr 47 SmC 74 N 91 I
3B7R	30	70	0	$9.9 \cdot 10^{-9}$	Cr 47 SmC 72 N 93 I
6OO8	0	100	0	$7.9 \cdot 10^{-9}$	Cr 41 SmC 50 N 89 I

increased. In the case of **6OO8**, according to our preliminary results obtained by a HP4194A Impedance gain-phase analyzer comparing the impedances of planar and homeotropic cells, the conductivity anisotropy is negligible at low frequencies (i.e. the parallel and the perpendicular components are almost the same), but becomes clearly positive at high frequencies.

The electroconvection measurements have been performed using either 20 μm thick commercial [31] or 13 μm thick homemade cells. Both cell types were constructed from glass substrates covered with etched indium tin oxide (ITO) electrodes and then with antiparallel rubbed polyimide layers to ensure planar orientation. The cells have been filled with the studied mixtures in the isotropic phase and then cooled down slowly to the nematic phase in order to obtain a well aligned sample. EC patterns have been induced by a sinusoidal AC voltage of variable frequency and amplitude which has been applied to the cells from a function generator (Agilent 33120A) through a high-bandwidth high-voltage amplifier. The patterns have been observed by polarizing optical microscopes (Leica DMR XP and Nikon OPTIPHOT-POL) under two crossed polarizers equipped with a digital CCD camera for recording snapshot images. Temperature has been controlled to a precision of 0.1 °C using a hot stage (Instec HS250).

III. DILUTION OF THE BANANA NEMATIC BY CALAMITIC MOLECULES

The EC scenarios have first been tested in 20 μm thick planar cells of the banana rich mixture **7B3R** in a very broad (10 Hz - 1 MHz) frequency range. The frequency dependence of the threshold voltage $U_c(f)$ of the patterns has been measured at three different temperatures: just below the clearing point ($T = 87^\circ\text{C} = T_{NI} - 1^\circ\text{C}$), in the middle of the nematic range at 82°C ($T_{NI} - 6^\circ\text{C}$), and also close to the nematic-smectic phase transition ($T = 72^\circ\text{C} = T_{NI} - 16^\circ\text{C}$). Here T_{NI} denotes the nematic-isotropic phase transition tempera-

ture. Patterns belonging to three different morphologies could be detected at each temperature. The frequency ranges for the occurrence of certain pattern types can easily be identified in the $U_c(f)$ plots shown in Fig. 2a, since the frequency dependence of U_c varies substantially from the morphological transitions. For comparison $U_c(f)$ of the pure **CIPbis10BB** is also reproduced from [5] in Fig. 2b.

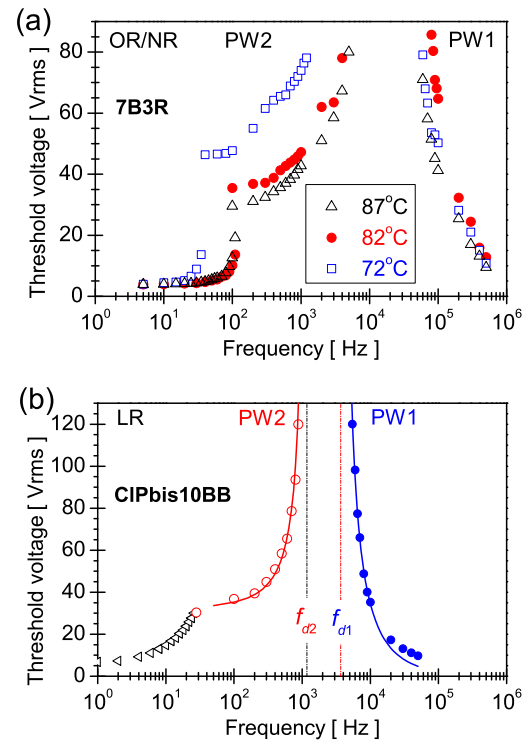


FIG. 2: (Color online) The threshold voltage $U_c(f)$ measured with crossed polarizers in (a) the mixture **7B3R** at 87°C ($T_{NI} - 1^\circ\text{C}$), 82°C ($T_{NI} - 6^\circ\text{C}$), and 72°C ($T_{NI} - 16^\circ\text{C}$) in a 20 μm thick planar cell; (b) in the pure **CIPbis10BB** at 75°C ($T_{NI} - 3^\circ\text{C}$) (from [5]). PW1 and PW2 denote the high f and the low f prewavy regimes, respectively.

At the lowest frequencies ($f \lesssim 100$ Hz) the typical roll patterns (OR or NR) of the conductive regime of standard EC have developed at U_c . Increasing the applied voltage slightly above threshold the roll patterns become modulated (Fig. 3a), forming zig-zag structures followed by defect chaos and dynamic scattering at high voltages.

Increasing f there is a crossover frequency f_c ($f_c \approx 110$ Hz at $T = T_{NI} - 6^\circ\text{C}$) where the morphology changes from conductive rolls to a prewavy pattern. In the close vicinity of f_c the two pattern types coexist in a form of a superposition (defect free chevron [32]). Above f_c two different regimes can be distinguished: one (PW2) at lower f up to a few kHz and another (PW1) at high f above 60 kHz. The appearance of the patterns in the two prewavy regimes is almost identical (compare Figs. 3b and 3c): they manifest themselves as wide stripes running normal to the rubbing direction; however, the frequency dependence of their threshold has an opposite slope (see Fig. 2a). In PW2 the threshold diverges with increasing frequency as $U_c(f) \propto (f_{d2} - f)^{-1}$, while in PW1 the divergence occurs at reducing the frequency as $U_c(f) \propto (f - f_{d1})^{-1}$ ($f_{d2} = 8.27$ kHz, $f_{d1} = 20.4$ kHz at $T = T_{NI} - 6^\circ\text{C}$). At voltages much above the threshold the prewavy pattern transforms into a 'wavy' one characterized by sinusoidally modulated disclination loops [11]. In the frequency band $f_{d2} < f < f_{d1}$ separating the two prewavy regimes no pattern has developed at all.

Comparing the behaviour of $U_c(f)$ measured at different temperatures (Fig. 2) one can notice that f_c , marking the crossover between NR and PW2, increases with raising the temperature. In the PW2 regime higher temperatures resulted in lower threshold voltages as well as in a shift of the lower divergence frequency f_{d2} to larger values. In contrast to that, in the PW1 neither the shift of U_c nor of the upper divergence frequency f_{d1} has exhibited a monotonic behaviour with the temperature variation.

For further characterization of the observed patterns their wavelengths λ have also been determined from snapshots taken at the onset. The dimensionless wave number $q_c^* = q_c d / \pi = 2d / \lambda$ [7] calculated from λ is presented in Fig. 4 for $T = 82^\circ\text{C} = T_{NI} - 6^\circ\text{C}$. At low frequencies $q_c^*(f)$ exhibited a monotonic increase with f ; growing sharply in the vicinity of f_c as expected for a conductive EC regime. In contrast to that, in the prewavy regimes $q_c^*(f)$ had a nearly constant value of about 0.8. It should be emphasized that no significant difference could be found between the q_c^* values of PW1 and PW2 apart from a very weak increase of q_c^* with f valid for both prewavy regimes.

The EC scenarios presented above strongly resemble those reported for the pure **CIPbis10BB** [5] and shown in Fig. 2b to allow easier comparison. Nevertheless two important differences have to be noticed. The first is a morphological difference: **7B3R** exhibits standard conductive rolls at low frequencies, in contrast to the non-standard longitudinal roll pattern of the pure banana nematic. The second is a difference in the frequency ranges.

Though the two prewavy regimes separated by a patternless frequency band do exist in **CIPbis10BB** as well as in the mixture **7B3R**, in the latter they occur at considerably higher frequencies, i.e. both f_{d2} and f_{d1} are about a decade larger in **7B3R** than in **CIPbis10BB**.

In order to investigate the influence of the further reduction of the concentration of the bent-core nematic on the EC scenarios, measurements have been carried out on $20\ \mu\text{m}$ thick cells filled with the more diluted mixtures of **5B5R** and **3B7R**, as well as on a $13\ \mu\text{m}$ thick cell of the pure **6O08**. The threshold voltages determined at $T_{NI} - 6^\circ\text{C}$ for all three compounds are presented in Figs. 5a-c together with snapshots of characteristic pattern morphologies in Figs. 5e-f. The $U_c(f)$ curve for **5B5R** shown in Fig. 5a still looks quite similar to that of the **7B3R**. The conductive rolls at $f \lesssim 150$ Hz followed by a prewavy pattern (PW2) up to 7 kHz do exist in **5B5R**; just f_c and f_{d2} are shifted to even higher frequencies compared to **7B3R**. The significant difference occurs at high frequencies. Though EC recovers above 100 kHz in **5B5R** too and its $U_c(f)$ curve decreases with f similarly to that of the PW1 regime in **7B3R**, the morphology of the pattern is completely different. In **5B5R** no prewavy pattern forms at high f , instead a dynamic EC pattern without any periodic stripe structure could be observed (see Fig. 5d). Moving to the mixture **3B7R** (which has even lower banana content) only the two low frequency pattern types, the conductive rolls and a prewavy pattern remain observable. It is seen in Fig. 5b that the crossover frequency shifted up to $f_c \approx 200$ Hz, but the $U_c(f)$ of the prewavy pattern grew much faster with f than in the previous compounds (the upper voltage limit of our amplifier has been reached at considerable lower frequencies) and was not describable by a hyperbolic divergence. The appearance of the prewavy pattern (Fig. 5e) was similar to that in the other mixtures and was characterized by similar $q_c^*(f) \approx 0.8$ values. In contrast to the previous mixtures no electroconvection could be detected above 1 kHz in **3B7R**.

Finally the pure calamitic **6O08** has also been tested and found to exhibit only standard EC. As seen in the $U_c(f)$ curve shown in Fig. 5c, the crossover from the conductive regime to the dielectric one occurs at about 200 Hz. The latter is characterized by a square root like $U_c(f)$ and the pattern at onset corresponds to very fine ($\lambda < 3\ \mu\text{m}$) dielectric rolls as shown in Fig. 5f. At high frequencies (above a few kHz) no EC could be detected. We should mention that, though no prewavy pattern could be observed in this sample, raising the voltage much above $U_c(f)$ in the dielectric regime the common dielectric chevron pattern (see Fig. 6) could be induced as a secondary instability. Although some characteristics of the dielectric chevrons (e.g. the azimuthal director modulation in the plane of the surfaces and the large secondary periodicity) may be similar to those of the prewavy pattern (compare Figs. 6ab with Figs. 3bc and 5e), they must not be mistaken. Dielectric chevrons occur as an ordering of defects in the dielectric roll structure (de-

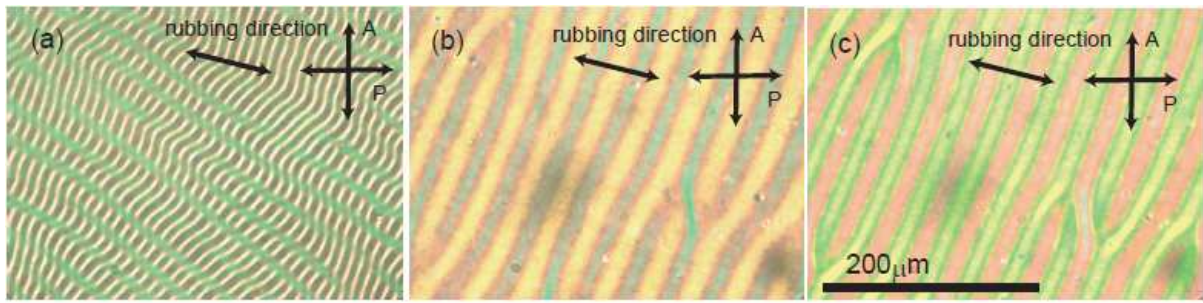


FIG. 3: (Color online) Snapshots of typical electroconvection patterns under crossed polarizers in the nematic phase of the mixture **7B3R** (1°C below the N-I transition). The rubbing direction of the $20\ \mu\text{m}$ thick planar cell made an angle of 20° with the polarizer. (a) Oblique rolls in the conductive regime at 4 Vrms, 10 Hz; (b) prewavy pattern in the PW2 regime at 50 Vrms, 200 Hz ($U_c = 31.1$ Vrms); (c) prewavy pattern in the PW1 regime at 40 Vrms, 200 kHz ($U_c = 25.4$ Vrms).

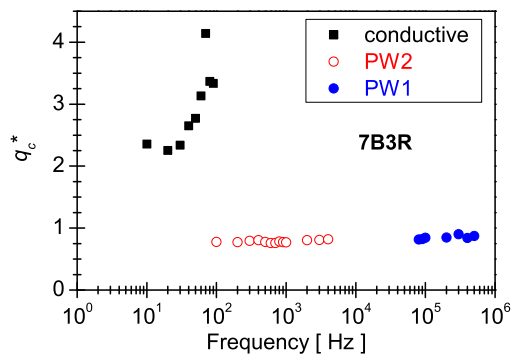


FIG. 4: (Color online) Frequency dependence of the dimensionless wave number q_c^* of the EC patterns in a $20\ \mu\text{m}$ thick planar cell of the mixture **7B3R**.

fect mediated chevrons [chevron]) where the initial rolls still remain detectable as demonstrated in Figs. 6a'b' using digital zooming. In contrast to that, rolls with a smaller wavelength have never been detected in the prewavy pattern.

IV. INFLUENCE OF THE CONDUCTIVITY

The studies presented above have convincingly shown that dilution of the bent-core with a calamitic nematic not only causes quantitative changes in the $U_c(f)$ behaviour, but affects the morphology and the existence of EC patterns. At the mixing the full set of material parameters (elastic moduli, viscosities, conductivity, etc.) changes therefore it is impossible to conclude which of those parameters is primarily responsible for the changes in the EC scenarios. One of them - the magnitude of the electrical conductivity σ_\perp - is, however, fairly easily controllable without affecting the other parameters via doping. Threshold voltages of EC patterns are known to be sensitive to the variation of the conductivity; this especially holds for the prewavy regime where a larger σ_\perp

promotes the occurrence of the pattern by reducing U_c . In addition it has been found that **6O08** had a smaller conductivity than **CIPbis10BB** (see Table I), so reduction of the banana content was always accompanied by a decrease of σ_\perp .

Based on these arguments we have decided to check the direct influence of the conductivity on the EC scenarios by doping the mixture **7B3R** with a conductive salt (**TBABE**, Fig. 1) in various concentrations. Figures 7b-d present the frequency dependence of the threshold voltages for **7B3R** doped with 0.01 wt%, 0.1 wt% and 1 wt% of **TBABE**, respectively. These measurements have been performed on $20\ \mu\text{m}$ thick planar cells in the middle of the nematic range at 80°C . In order to make comparison easier we have added $U_c(f)$ of the undoped **7B3R** obtained at 82°C in Fig. 7a. It is common for all four compositions that they exhibit both conductive rolls and prewavy pattern. Increasing the dopant concentration and thus σ_\perp the crossover between the two pattern types shifts toward higher frequencies considerably (from 110 Hz to 13 kHz); this corresponds to the expected behaviour. In the doped samples a slight increase of U_c could be detected when $f \rightarrow 0$, which becomes more pronounced at the highest (1 wt%) doping concentration (Fig. 7d). We suggest that this unusual behaviour might be related to a big space charge polarization induced by the large number of ions generated by the added salt [33, 34], which may disturb the electroconvective pattern formation.

Doping influences heavily the prewavy regimes too. In the undoped **7B3R** the PW2 and PW1 regimes are clearly separated by a patternless frequency band due to the divergences of $U_c(f)$ (Fig. 7a). In contrast to that, already the lowest (0.01 wt%) dopant concentration makes the prewavy threshold curve continuous (Fig. 7b), i.e. the divergences tame down to a maximum. A stronger doping (0.1 wt%) reduces the prewavy thresholds and lowers the maximum value further (Fig. 7c). Finally at 1 wt% doping the maximum is fully suppressed and $U_c(f)$ becomes flat in the whole prewavy range (Fig. 7d).

In the pure **CIPbis10BB** it has been found that the temperature dependence of U_c near the clearing point is

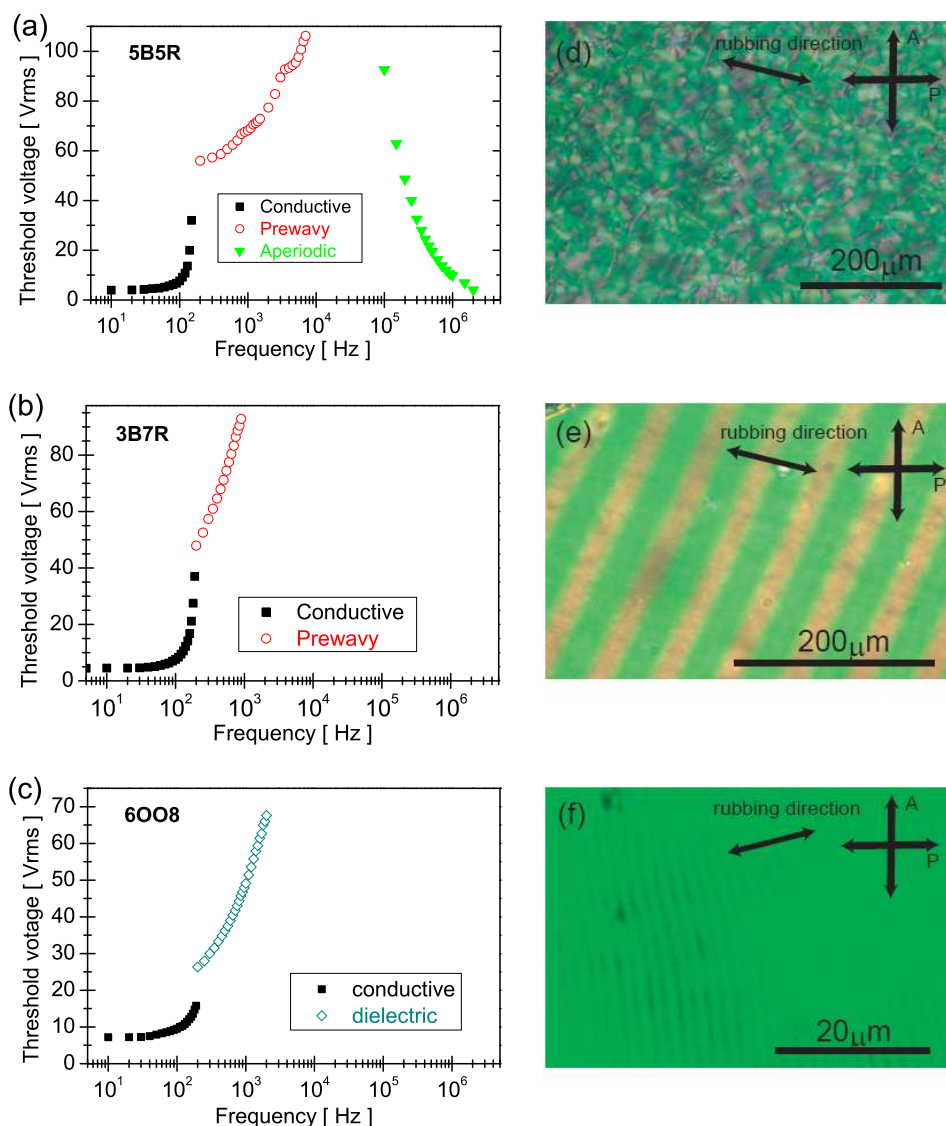


FIG. 5: (Color online) Frequency dependence of the EC threshold voltage $U_c(f)$ and typical EC patterns in the middle of the nematic phase ($T = T_{NI} - 6^\circ\text{C}$) (a) in the mixture **5B5R** featuring conductive rolls, prewavy pattern and a dynamic aperiodical convection; (b) in the mixture **3B7R** featuring conductive rolls and prewavy pattern but no EC at high frequencies; (c) in the pure calamitic **6008** featuring conductive rolls and dielectric rolls but no EC at high frequencies. Snapshot photomicrographs of typical EC patterns at onset taken at crossed polarizers: (d) a dynamic aperiodical convection at 55 Vrms, 500 kHz in **5B5R**; (e) the prewavy pattern at 60 Vrms, 250 Hz in **3B7R**; (f) dielectric rolls at 42 Vrms, 500 Hz in **6008**. Please, note the changes in the magnification as marked by the scale bars.

different in the two prewavy modes (PW2 and PW1) occurring in distinct frequency ranges [5]. This fact has led to the conclusion that the otherwise similar prewavy patterns in these two regimes may be the result of different pattern forming mechanisms whose details still await for exploration. On this ground we have carried out similar studies on the temperature dependence in the undoped and the 0.1 wt% doped **7B3R**. In the undoped **7B3R** $U_c(T)$ has been measured at two selected frequencies: at 200 Hz in PW2 and at 200 kHz in PW1 (Fig. 8a). While $U_c(T)$ in PW1 possessed a maximum

near the middle of the nematic range, the same in PW2 exhibited a monotonic decrease with an indication of a possible minimum near T_{NI} . This behaviour resembles that of the pure **CIPbis10BB** (see Fig. 9 of [5]) though the change in dU_c/dT for PW1 near the phase transition is much less pronounced in **7B3R**. In **7B3R** doped with 0.1 wt% **TBABE** prewavy patterns occur only at higher frequencies and there is no frequency band without pattern. Here the temperature dependence of the onset voltage at frequencies selected from both sides of the maximum of $U_c(f)$, 50 kHz and 250 kHz, have been com-

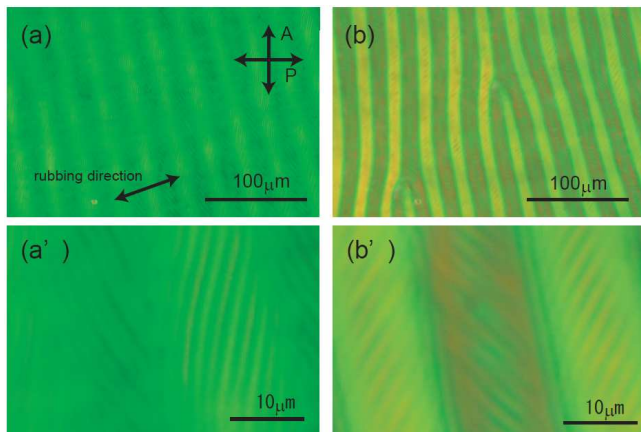


FIG. 6: (Color online) Photomicrographs of the dielectric chevrons in a $13 \mu\text{m}$ thick planar cell of the pure rod-like nematic **6008** at 80°C taken under cross polarizers at applied voltages of (a) 46 Vrms, 500 Hz and (b) 49 Vrms, 500 Hz ($U_c = 36.2$ Vrms). Images (a') and (b') are digitally zoomed sections of (a) and (b), respectively, in order to demonstrate the presence of the initial fine dielectric rolls.

pared in Fig. 8b. Similarly to Fig. 8a, $U_c(T)$ expresses a maximum for the higher frequency while a monotonic decrease is found for the lower frequency, but the change in dU_c/dT close to T_{NI} seems to fade away. Thus based on the above measurements we can neither prove nor exclude that in the studied mixtures the lower frequency ($dU_c/df > 0$) and the higher frequency ($dU_c/df < 0$) prewavy regimes are the results of different pattern forming mechanisms.

V. DISCUSSION AND CONCLUSIONS

During the long history of EC in calamitic nematics experimental studies have mainly been carried out in the frequency range below 20 kHz. Only a few measurements have been extended to higher frequencies including investigations on the prewavy pattern in highly conductive MBBA [35] or on the behaviour of bent-rod twin mesogen with dielectric inversion [26, 27]. For all pattern morphologies of standard EC (conductive or dielectric rolls) described by the SM [6, 8] as well as for the nonstandard longitudinal rolls explained recently by incorporating the flexoelectric effects [23] the theory predicts threshold voltages growing with the frequency ($dU_c/df > 0$). These predictions have fully been confirmed by experiments, apart from a low f anomaly in the dielectric regime observed recently in very thin cells [36]. Moreover, $dU_c/df > 0$ has been experimentally found for the prewavy pattern too [15, 16] and as far as we know the same is predicted by all theoretical models of other EC modes [37, 38]. The lack of high frequency studies thus might have practical reasons. Whenever $U_c(f)$ has raised above the upper voltage limit of the available amplifiers, the pattern could not be excited anymore; neither

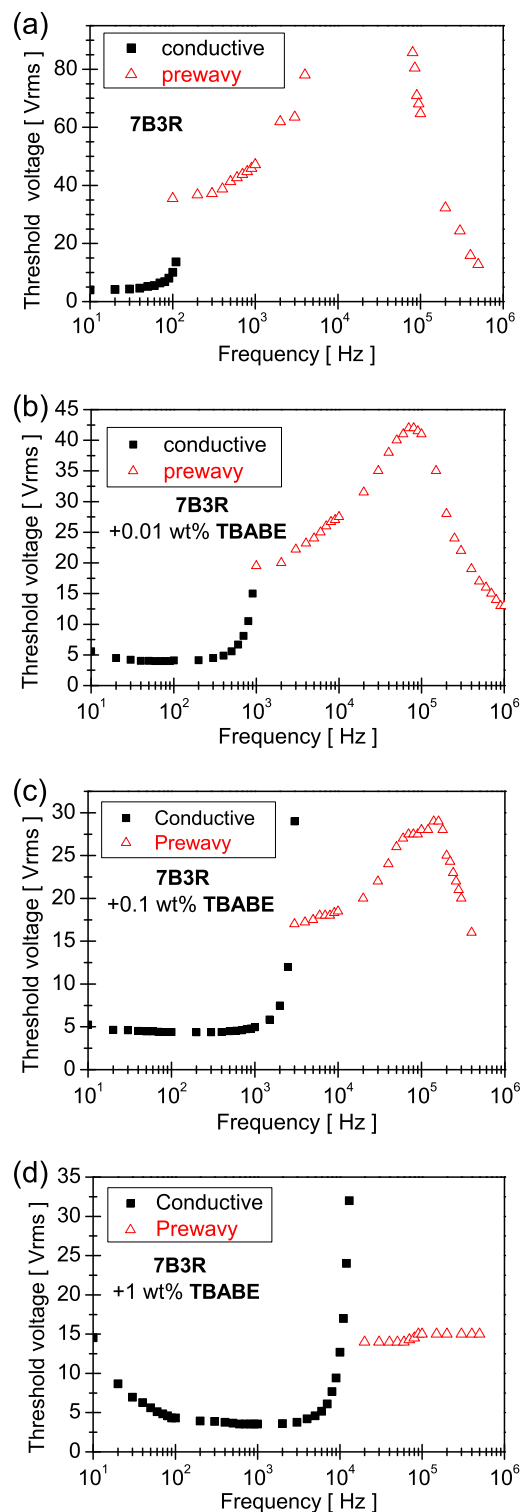


FIG. 7: (Color online) Frequency dependence of the threshold voltage $U_c(f)$ for the (a) undoped **7B3R** at 82°C ; (b) **7B3R** doped with 0.01 wt% of **TBABE** at 80°C ; (c) **7B3R** doped with 0.1 wt% of **TBABE** at 80°C ; (d) **7B3R** doped with 1 wt% of **TBABE** at 80°C .

was it expected to reappear again at higher f due to the

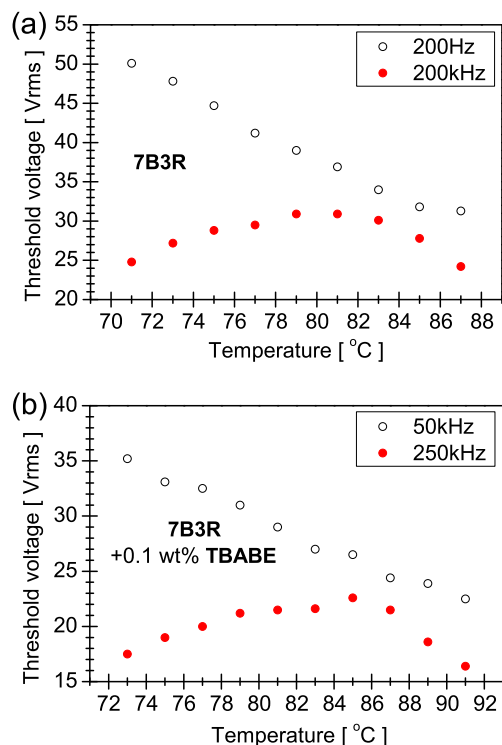


FIG. 8: (Color online) Temperature dependence of the threshold voltage $U_c(T)$ at two frequencies selected from the lower and the higher frequency part of the prewavy regime, respectively, for (a) the undoped mixture **7B3R** and (b) the mixture **7B3R** doped with 0.1 wt% **TBABE**.

positive slope of $U_c(f)$.

The existence of EC patterns with relatively low threshold at extremely high frequencies seems to be related to bent core nematics [5, 24] like **CIPbis10BB**. Their peculiarity is that they possess a high frequency prewavy regime (PW1) characterized by the unprecedented $dU_c/df < 0$ besides another, low f prewavy regime (PW2) of the common $dU_c/df > 0$. The regimes with opposite slope of $U_c(f)$ are assumed to be results of different, though yet undiscovered, pattern forming mechanisms. This behaviour abides only in the banana rich **CIPbis10BB/6OO8** mixtures (**7B3R**), but fades away at increasing concentration of the calamitic component; furthermore no PW1 like patterns have been known in calamitic compounds yet. These facts lead to the conclusion that the existence of the dual prewavy regime and especially that of the PW1 mode with $dU_c/df < 0$ might be related to the combination of the extraordinary molecular structure and material parameters [40] of the bent-core nematic.

Moreover, we have shown in the doping experiments

that the PW1 region tends to disappear with increasing conductivity. In the pure **CIPbis10BB** and in the undoped **7B3R** the threshold voltages for both PW2 and PW1 diverge enclosing a frequency band $f_{d2} < f < f_{d1}$ with an infinite pattern threshold (see Figs. 2ab and 7a). Increasing the conductivity may shift the divergence frequencies of the individual modes or weaken their diverging tendency, leading to a turnover $f_{d1} < f_{d2}$. Then the two threshold curves would cross and a change from PW2 to PW1 could occur at finite U_c at a crossover frequency ($\approx 10^5$ Hz) as seen in Fig. 7b. Increasing the conductivity further (Fig. 7c) the crossover frequency shifts to higher values while the threshold decreases, reaching finally a state with a flat $U_c(f)$ in Fig. 7d. Hence the initially higher conductivity of the bent-core nematic compared with that of the calamitic compound (Table I) cannot be the cause for the emergence of PW1 with $dU_c/df < 0$. On the contrary, the findings could rather be formulated in a way that the effect of the banana shaped molecules on the EC threshold is suppressed by the increased conductivity.

It should be mentioned that going from Fig. 7a to Fig. 7d the conductivity has been increased enormously, by 3 orders of magnitude, which shows up also in the shift of the cutoff frequency of the conductive EC regime by about two orders of magnitude.

In order to interpret the detected behaviour one can either think of new mechanisms, not included into the standard model (like an isotropic mechanism [38], a special consequence of the unusually large flexoelectric coefficients, electrolytic effects due to the high conductivity [39], etc.), or one could also consider to stay within the frame of the standard model and preserve the inertial term ($\propto f^2$) in the nematohydrodynamic equations [38], which is usually neglected in the theoretical description. Here it might have a relevance due to the extreme high ($f > 100$ kHz) frequencies of the PW1 mode.

Acknowledgments

The authors thank to T. Tóth Katona and J.T. Gleeson for fruitful discussions. Financial support by the Hungarian Research Fund OTKA-K61075 and the Grant-in-Aid for Scientific Research (S) (16105003) from the Ministry of Education, Culture, Science, Sports and Technology of Japan are gratefully acknowledged. S.T. and N.É., K.F.-Cs. are grateful to the hospitality provided by the Research Institute for Solid State Physics and Optics, Budapest and the Tokyo Institute of Technology, respectively, within the framework of a bilateral joint project of the Japanese Society for the Promotion of Sciences and the Hungarian Academy of Sciences.

[1] H. Takezoe, and Y. Takanishi, Jpn. J. Appl. Phys. **45**, 597 (2006).

[2] L.A. Madsen, T.J. Dingemans, M. Nakata, and E.T.

- Samulski, Phys. Rev. Lett. **92**, 145505 (2004).
- [3] B.R. Acharya, A. Primak, and S. Kumar, Phys. Rev. Lett. **92**, 145506 (2004).
- [4] J. Harden, B. Mbanda, N. Éber, K. Fodor-Csorba, S. Sprunt, J.T. Gleeson, and A. Jákli, Phys. Rev. Lett. **97**, 157802/1-4 (2006).
- [5] D. B. Wiant, J. T. Gleeson, N. Éber, K. Fodor-Csorba, A. Jákli, and T. Tóth-Katona, Phys. Rev. E **72**, 041712/1-12 (2005).
- [6] L. Kramer and W. Pesch, In *Physical Properties of Liquid Crystals: Nematics*, editors: D.A. Dunmur, A. Fukuda and G.R. Luckhurst, (Inspec, London, 2001), pp. 441-454.
- [7] Á. Buka, N. Éber, W. Pesch, and L. Kramer: In *Self-Assembly, Pattern Formation and Growth Phenomena in Nano-Systems*. Eds. A. A. Golovin, A. A. Nepomnyashchy, NATO Science Series II, Mathematica, Physics and Chemistry, Vol. 218, (Springer, Dordrecht, 2006), pp. 55-82.
- [8] L. Kramer and W. Pesch, In *Pattern Formation in Liquid Crystals*, editors: A. Buka and L. Kramer, (Springer, New York, 1996), pp. 221-255.
- [9] M. May, W. Schöpf, I. Rehberg, A. Krekhov, and A. Buka, Phys. Rev. E **78**, 046215 (2008).
- [10] Á. Buka, P. Tóth, N. Éber, and L. Kramer, Physics Reports **337**, 157-169 (2000).
- [11] S. Kai, and K. Hirakawa: Solid State Comm. **18**, 1573 (1976).
- [12] P. Petrescu, and M. Giurgea: Phys. Lett. A **59**, 41 (1976).
- [13] A.N. Trufanov, M.I. Barnik and L.M. Blinov, In *Advances in Liquid Crystal Research and Application*, editor: L. Bata, (Akademiai Kiad, Budapest - Pergamon Press, New York, 1980), pp. 549-560.
- [14] L. Nasta, A. Lupu, and M. Giurgea, Mol. Cryst. Liq. Cryst. **71**, 65 (1981).
- [15] J.-H. Huh, Y. Hidaka, Y. Yusril, N. Éber, T. Tóth-Katona, Á. Buka, and S. Kai, Mol. Cryst. Liq. Cryst. **364**, 111-122 (2001).
- [16] J.-H. Huh, Y. Yusuf, Y. Hidaka, S. Kai, Phys. Rev. E **66**, 031705 (2002).
- [17] J.-H. Huh, Y. Yusuf, Y. Hidaka, and S. Kai, Mol. Cryst. Liq. Cryst. **410**, 39 (2004).
- [18] N. Éber, and Á. Buka, Phase Transitions **78**, 433-442 (2005).
- [19] M. Goscianski and L. Léger, J. Phys. (Paris) **36**, N.3, C1-231 (1975).
- [20] L.M. Blinov, M.I. Barnik, V.T. Lazareva and A.N. Trufanov, J. Phys. (Paris) **40**, N.4, C3-263 (1979).
- [21] E. Kochowska, S. Németh, G. Pelzl and Á. Buka, Phys. Rev. E **70**, 011711 (2004).
- [22] T. Tóth-Katona, A. Cauquil-Vergnes, N. Éber, and Á. Buka, Phys. Rev. E **75**, 066210/1-12 (2007).
- [23] A. Krekhov, W. Pesch, N. Éber, T. Tóth-Katona, and Á. Buka, Phys. Rev. E **77**, 021705/1-11 (2008).
- [24] S. Tanaka, S. Dhara, B.K. Sadashiva, Y. Shimbo, Y. Takanishi, F. Araoka, K. Ishikawa, and H. Takezoe, Phys. Rev. E **77**, 041708 (2008).
- [25] J. Heuer, R. Stannarius, M.-G. Tamba, and W. Weissflog, Phys. Rev. E **77**, 056206 (2008).
- [26] P. Kumar, U.S. Hiremath, C.V. Yelamaggad, A.G. Rossberg, and K.S. Krishnamurthy, J. Phys. Chem. B **112**, 9270-9274 (2008).
- [27] P. Kumar, U.S. Hiremath, C.V. Yelamaggad, A.G. Rossberg, and K.S. Krishnamurthy, J. Phys. Chem. B **112**, 9753-9760 (2008).
- [28] K. Fodor-Csorba, A. Vajda, G. Galli, A. Jákli, D. Demus, S. Holly, and E. Gács-Baitz, Macromol. Chem. Phys. **203**, 1556 (2002).
- [29] G.G. Nair, C.A. Bailey, S. Taushanoff, K. Fodor-Csorba, A. Vajda, Z. Varga, A. Bóta, and A. Jákli, Adv. Mater. **20**, 3138-3142 (2008).
- [30] J.P. van Meter, and B.H. Klanderma, Mol. Cryst. Liq. Cryst. **22**, 271 (1973).
- [31] Cells supplied by Z. Raszewski, Military Technical Academy, Warsaw.
- [32] J.-H. Huh, Y. Hidaka, A.G. Rossberg and S. Kai, Phys. Rev. E **61**, 2769 (2000).
- [33] A. Sawada, Y. Nakazono, K. Tamuri, and S. Naemura, Mol. Cryst. Liq. Cryst. **318**, 225 (1998).
- [34] A. Sawada, K. Tamuri, and S. Naemura, Jpn. J. Appl. Phys. **38** 1418 (1999).
- [35] A.N. Trufanov, L.M. Blinov, and M.I. Barnik, Zh. Eksp. Teor. Fiz. **78**, 622 (1980).
- [36] T. Tóth-Katona, N. Éber, Á. Buka, and A. Krekhov, Phys. Rev. E. **78**, 036306/1-12 (2008).
- [37] L.M. Blinov, and V.G. Chigrinov, *Electrooptic Effects in Liquid Crystal Materials*, (Springer, New York, 1996).
- [38] S.A. Pikin, *Structural Transformations in Liquid Crystals*, (Gordon and Breach, New York, 1991).
- [39] Treiber M. and Kramer L., Mol. Cryst. Liq. Cryst. **261** (1995) 311.
- [40] A. Jákli, M. Chambers, J. Harden, M. Madhabi, R. Teeling, J. Kim, Q. Li, G.G. Nair, N. Éber, K. Fodor-Csorba, J.T. Gleeson, and S. Sprunt, In *Proceedings of Emerging Liquid Crystal Technologies III, San Jose, January 20-24, 2008*, Proc. SPIE Vol. **6911**, 691105/1-10 (2008).